UDC 530.311

Gavrilov S.V., Kharitonov A.L. A plate tectonic model for the origin of metal provinces in Amur region of Asian lithospheric plate and subduction convective mechanism of the dissipative heat and calcareous-alcaline magmas upward transport from the mantle wedge

Gavrilov Sergei Vladilenovich,
Doctor of physical and mathematical sciences, Main scientist of the laboratory 102, Schmidt Institute of Physics of the Earth of the Russian Academy of Sciences
Kharitonov Andrey Leonidovich,
Candidate of physical and mathematical sciences, Leading scientist of the Main Earth's magnetic field laboratory, Pushkov Institute of Terrestrial Magnetism, Ionosphere and Radio Waves Propagation of the Russian Academy of Sciences

Abstract. *For the mantle rheology case the thermal viscous dissipation-driven thermal convection in the mantle wedge above the Amur Lithospheric Plate subducting under the Okhotsk Lithospheric Plate is modeled numerically. Within the framework of the model constructed the horizontal extent and localization of the 2D heat flux anomaly observed in the Okhotsk Sea eastward of the Sakhalin Island correspond to subduction velocity ~ 10 mm a year which is close to that observed with the geodetic means. For non-Newtonian rheology the model heat flux anomaly is ~ 130 mW×m^{-2} which fits well to the observed 2D heat flux anomaly. Rheological constants of the mantle wedge material are specified more accurately, the concentration of water in the mantle wedge being ~ 1 wt. %. The effects of the 410 km and 660 km phase transitions are taken into account. A comparison of the model scales and locations of convective flows in the mantle wedge for the cases of continental and oceanic types of Okhotsk Lithospheric Plate serves as the evidence in favor of the former (continental) type of Okhotsk Lithospheric Plate. Upwelling mantle wedge convective flow is indicated to be able to provide the mantle wedge calcareous-alkaline magmas transport to the Earth's surface. The ascending convective movements in the mantle can take out mantle calcareous-alkaline magmas (with the metal ores which are contained in them) to the Earth's surface, and, therefore, ore deposits probably have to be dated for zones of the raised heat flux, located over convective Karig flows.*

Keywords: *tectonic model, mantle wedge thermal convection, calcareous-alkaline magmas transport, subduction angle and velocity, mantle rheology, metal provinces.*

Introduction

The problem of origin of metal provinces is discussed by the number of american scientists [12; 14; 17]. Some geologists [12; 14; 17] regard the spatial distribution of the metal provinces as reflecting the heterogeneities in the distribution of metals in the upper mantle (Fig. 1).

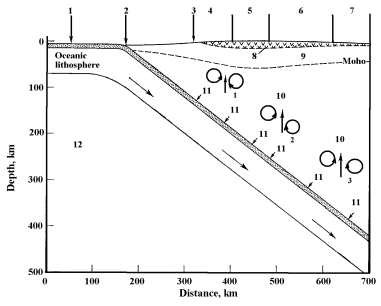

Fig. 1. Schematic deep section of a typical subduction zone showing the surface distribution of the metal provinces (4-7) above the several pairs of the Karig

thermodynamic convective vortices (10) over the subducting slab. The metals-containing calcareous-alkaline magmas entrained in the upwelling mantle flows (shown by vertical arrows) provide the formation of the subsurface ore deposits in the Earth's crust [17]. 1 – oceanic crust and lithosphere; 2 – oceanic trench; 3 – coast of the continental lithospheric plate; 4 – zone of accumulation of iron-containing ores; 5 – zone of accumulation of ores containing gold (Au) and copper (Cu); 6 - zone of accumulation of ores containing silver (Ag), lead (Pb), zinc (Zn); 7 - zone of accumulation of ores containing tin (Sn), molybdenum (Mo); 8 - sedimentary layer; 9 - zone of calcareous-alkaline intrusions (plutons) and volcanic rocks; 10 - zone of rise of calcareous-alkaline magmas and metals contained in them; 11 - partial melting in the absorption zone of oceanic crust layers and metals contained therein; 12 – asthenosphere.

The purpose of this article is to try from the perspective of the concept of lithospheric plate tectonics [12; 14; 17] to explain the origin of some metal provinces of the Far East of the Eurasian plate. Except for the three main lithospheric plates in the Far East of North Asia, viz. the Eurasian, Pacific and North American ones, there are the following plates: the Amur, Okhotsk ones, the concept of the former of which (Amur) was for the first time grounded in [24].

The localization and nature of the boundary between the Amur and Okhotsk Lithospheric Plates became recently a matter of ambiguous and sometimes contradictory debates [18]. According t\o the latter publication as well as to [6] the Sakhalin island belongs to the active region of North-Eastern Asia, the Sakhalin Island itself being the territory comprising the boundary between the largest lithospheric plates of the Earth, viz. the Eurasian, North-American and Pacific ones. Along the convergent boundaries of these plates there lies a broad boundary zone represented by the Amur, Okhotsk Lithospheric Plates, the two biggest of which (the Amur and Okhotsk ones) being separated by the great Central-Sakhalin (Tym-Poronaysk) fault. Arguments in [20; 21] support the idea of the eastward subduction of Amur Lithospheric Plate under the Okhotsk one with a velocity of ~10 mm per year. According to [10] the Sakhalin Island moves to the west with the velocity of 3 – 4 mm per year with respect to the Eurasian Lithospheric Plate, while the Sakhalin eastward velocity relatively to North America amounts to 3 – 5 mm per year. In [10] the GPS observational data collected in the Far East for over 10 years are as well indicated to support the eastward subduction of the Amur Lithospheric Plate under the Okhotsk one at the fault bisecting the Sakhalin Island. According to seismic data the subduction angle is equal to 36º, however, the abovementioned inter seismic GPS data can be interpreted, although with less grounds, in favor of the western subduction of Okhotsk Lithospheric Plate under the Amur one at an angle of ~ 45º (see Table 1 in [10]). It is worth noting that in [8] the boundary between the Amur and Okhotsk Plates is reported to be "the boundary of ambiguous nature", while in [16] the boundary between the Amur and Okhotsk Lithospheric Plates is considered to bisect the Sakhalin Island,

where numerous shallow micro earthquakes occur. The predominant geological structures there are those corresponding to the tectonics of compression, such as faults and folds of the north – south orientation, directed along the longitudinal axis of the Sakhalin Island. One of the main faults is the Central-Sakhalin one, which is a thrust fault of the meridian orientation, falling down to the west at an angle of approximately 70º. This may be regarded as just another indication by the authors of [8] (and the authors referred to in op. cit.) to the sufficiently steep subduction of the Okhotsk Lithospheric Plate under the Amur one in the western direction.

The goal of the present research is modeling the convective mass- and dissipative heat transfer from the mantle wedge above the subducting Amur Lithospheric Plate to the Earth's surface. Modeling of the localization and transversal horizontal extent of the 2D zone of anomalous heat flux at the Okhotsk seafloor eastward off the Sakhalin Island (as well as of the heat flux maximum absolute value) allows reliable evidencing in support of the amplitude and eastern direction of the Amur Lithospheric Plate subduction velocity. The model constructed here indirectly confirms the non-Newtonian mantle rheology to predominate in the mantle wedge sufficiently saturated with water, extracted from a subducting lithospheric plate, increasingly compressed in the course of subduction.

According to [2; 4; 5], two types of dissipation-driven small-scale thermal convection in the mantle wedge are possible, viz. the 3D finger-like convective jets, raising to volcanic chain, and the 2D transversal Karig vortices [7], aligned perpendicularly to subduction. These two types of convection are shown to be spatially separated due to the pressure and temperature dependence of mantle effective viscosity, the Karig vortices, if any of them formed, being located behind the volcanic arc [2]. Since there is a lack of unambiguous understanding of the plates subduction in the area of Sakhalin, the present modeling of distribution and absolute value of the anomalous heat flux from the Okhotsk seafloor is all the more important, as it may serve as a decisive argument favoring the eastward subduction of the Amur Lithospheric Plate. Numerical modeling of 2D mantle convection, occurring in the Karig vortices form and transporting dissipative heat, may allow judging about the mean water content in the mantle wedge as well as about the convective transport of mantle hydrocarbons to the Okhotsk seafloor. The model of convection presented here takes into account the temperature and pressure dependence of viscosity and fits best to observations in the case of non-Newtonian rheology for the mean water content of ~ 1 wt. % and subduction velocity of ~ 10 mm per year. In [23] such a great (and even several times greater) water content is indicated as possible to be observed in the transition zone of a mantle wedge.

Materials and Methods

Thermo-tectonic model of the mantle wedge between the base of overlying Okhotsk Lithospheric Plate and the upper surface of Amur Lithospheric Plate subducting under the Okhotsk one with a velocity V at an angle β is obtained for

the infinite Prandtl number fluid as a solution of non-dimensional 2D hydrodynamic equations in the Boussinesq approximation for a streamfunction ψ and temperature T [15]:

$(\partial^2_{zz}-\partial^2_{xx})\times\eta\times(\partial^2_{zz}-\partial^2_{xx})\times\psi+4\times\partial^2_{xz}\eta\times\partial^2_{xz}\psi=Ra\times T_x-Ra^{(410)}\times\Gamma_x^{(410)}-Ra^{(660)}\times\Gamma_x^{(660)}$, (1)

$\partial_t T = \Delta T - (\psi_z \times T_x) + (\psi_x \times T_z) + (Di / Ra) \times (\tau^2_{ik} / 2 \times \eta) + Q$, (2)

Here η is dynamic viscosity, ∂ and indices denote partial derivatives with respect to coordinates x (horizontal), z (vertical) and time t, Δ is the Laplace operator, $\Gamma_x^{(410)}$ and $\Gamma_x^{(660)}$ are volumetric ratios of the heavy phase at the 410 km and 660 km phase boundaries, the velocity components V_x and V_z are expressed through ψ as

$$V_x = \psi_z \ , \quad V_z = -\psi_x \ , \tag{3}$$

while non-dimensional Rayleigh number Ra, phase numbers $Ra^{(410)}$, $Ra^{(660)}$ and dissipative number Di are

$Ra=[(\alpha\times\rho\times g\times d^3\times T_1)/(\eta_C\times\chi)]=6.62\times10^8$; $Ra^{(410)}=[(\delta\rho^{(410)}\times g\times d^3)/(\eta_C\times\chi)]= 7.87\times10^8$;

$Ra^{(660)} = [(\delta\rho^{(660)}\times g\times d^3) / (\eta_C \times\chi)] = 10.0\times10^8$; $Di = [(\alpha \times g\times d) / c_p] = 0.175$, (4)

where $\alpha = 3\times10^{-5}$ K^{-1} is the thermal expansion coefficient, $\rho = 3.3$ g·cm^{-3} is the density, g is gravity acceleration, $c_p = 1.2\times10^3$ J · kg^{-1}·K^{-1} is specific heat capacity at constant pressure, $T_1 = 1950^o$K is the temperature at the base of the mantle transition zone (MTZ) at the depth of 700 km regarded as the lower boundary of the model domain, $Q = 6.25\times10^{-4}$ mW·m^{-3} is the volumetric heat generation in the crust, τ_{ik} is the viscous stress tensor, d = 700 km is the vertical dimension of the modeled domain, $\eta_C = 10^{18}$ Pa · s is the viscosity scaling factor, $\chi = 1$ mm^2 · s^{-1} is thermal diffusivity, $\delta\rho^{(410)} = 0.07\rho$ and $\delta\rho^{(660)} = 0.09\rho$ are the density changes at the 410 km and 660 km phase boundaries respectively. In (1), (2) the scaling factors for time t, coordinates x and z, stresses τ_{ik}, and the stream-function ψ are ($d^2 \times\chi^{-1}$), d, ($d^{-2}\times\eta_C \times \chi$) and χ respectively. Assuming rheology be linear for the diffusion creep deformation mechanism dominating in the mantle at depths over ~ 200 km [1], we accept the temperature- and lithostatic pressure p dependent viscosity as [23]

$$\eta = (\mu / 2 \times A) \times (C_w^r \times\tau^{n-1}) \times (h / b^*)^m \times\{ \exp [(E^* + p\times V^*) / (R \times T)] \}, \tag{5}$$

where for "wet" olivine $A = 5.3\cdot10^{15}$ s^{-1}, m = 2.5, the grain size $h = 10^{-1}$ – 10 mm, $b^* = 5\cdot10^{-8}$ cm is the Burgers vector [23], $E^* = 240$ kJ·mol^{-1} is activation energy, $V^* = 5\times10^3$ mm^3·mol^{-1} is the activation volume, $\mu = 300$ GPa is the shear modulus normalizing factor, R is the gas constant. At the constants chosen and the grain size h =1.6 mm, non-dimensional viscosity also denoted η is

$$\eta = (5.00 \times 10^{-7}) \times \exp \{[14.80 + 6.72 \times (1 - z)] / T\} , \tag{6}$$

where T is non-dimensional temperature, non-dimensional z normalized by d is pointing upwards from the MTZ base and x is pointing against subduction along the MTZ base. The aspect ratio of the model domain is 1:1.723 thus the subduction angle being $\beta = 30°$ if subduction is assumed to take place along the model domain diagonal. Non-dimensional trial subduction velocity V = 10 mm·a^{-1} normalized by ($d^{-1}\times\chi$) equals $V = 0.208\cdot10^3$, i.e. non-dimensional velocity components of

subducting Amur Lithospheric Plate are $V_x = -0.1914 \cdot 10^3$ и $V_z = -0.1105 \cdot 10^3$. To check as to how the estimate of velocity of subduction of the Amur Lithospheric Plate is sensitive to the accepted linear rheological law here we make extra computations for non-Newtonian rheology, in which case the viscosity formulae (5)–(6) are rewritten as

$$\eta = (1 / 2 \times A \times C_w^r \times \tau^{n-1}) \times (h / b^*)^m \times \{\exp [(E^* + p \times V^*) / (R \times T)]\}, \quad (7)$$

where according to [22] for "wet" olivine $n = 3$, $r = 1.2$, $m = 0$, $\tau = (\tau_{ik}^2)^{1/2}$, $E^* = 480$ kJ·mol^{-1}, $V^* = 11 \times 10^3$ mm^3·mol^{-1}, $A = 10^2$ c^{-1}×(MPa)$^{-n}$, $C_w > 10^{-3}$ for "wet" olivine is the weight water concentration (in %). It should be noted the constants in (7) vary considerably in the papers referred to by [22] and heretofore we gave averaged values of constants.

At $C_w = 10^{-3}$ on accounting for

$$\tau_{ik}^2 = (4 \times \eta^2) \times [(\psi_{zz} - \psi_{xx})^2 / 2 + 2 \times \psi^2_{xz}], \quad (8)$$

non-dimensional viscosity is

$$\eta = \{1.27 / [(\psi_{zz} - \psi_{xx})^2 / 2 + 2 \times \psi^2_{xz}]^{1/3}\} \times \exp \{[10.0 + 5.3 \times (1 - z)] / T\} \quad (9)$$

It should be explained why the angle of subduction $\beta = 30°$ is taken here to be less than the angle $\beta = 36°$, which follows from the seismic observational data in [10]. The point is that in [11] the additional right-lateral strike slip plates motion is shown to take place at the thrust Central-Sakhalin predominantly normal fault at the velocity ~ 6 times less than the velocity of subduction. As a consequence, the motion of mantle material in the mantle wedge, aroused by mutual movements of Amur and Okhotsk Lithospheric Plates, occurs along some tilted direction rather than exactly perpendicularly to the Central-Sakhalin fault, and the angle within which the mantle material motion is comprised in the mantle wedge, is by a factor of 5/6 sharper than that, corresponding to seismic data, i.e. equals $\beta = 30°$.

Following [22] we assume the phase functions $\Gamma^{(l)}$ as

$$\Gamma^{(l)} = (1/2) \times \{1 - th [z - z^{(l)}(T)] / w^{(l)}\}; \; z^{(l)}(T) = z_o^{(l)} - \{[\gamma^{(l)} \times (T - T_o^{(l)})] / (\rho \times g)\}, \quad (10)$$

where the signs are changed as z-axis is pointing upwards, $z^{(l)}(T)$ is the depth of the l-th phase transition (l = 410, 660), $z_0^{(l)}$ and $T_0^{(l)}$ are the averaged depth and temperature of the l-th phase transition, $\gamma^{(410)} = 3$ MPa×K^{-1} and $\gamma^{(660)} = -3$ MPa×K^{-1} are the slopes of the phase equilibrium curves, $w^{(l)}$ is the characteristic thickness of the l-th phase transition, $T_0^{(410)} = 1800^oK$, $T_0^{(660)} = 1950^oK$ are the mean phase transition temperatures. The heats of phase transitions are neglected in (2) as insignificant in the case of developed convection as in [22]. From (10) it follows

$$\Gamma_x^{(l)} = - (\gamma^{(l)} / 2 \times \rho \times g \times w^{(l)}) \times T_x \times ch^{-2} \{[(z - z_o^{(l)} + \gamma^{(l)} \times (T - T_o^{(l)})) / (\rho \times g)] / w^{(l)}\}, \quad (11)$$

wherefrom it is clear the phase transition with $\gamma^{(l)} > 0$ facilitates convection (at l = 410), while the phase transition with $\gamma^{(l)} < 0$ hinders convection (at l = 660). In non-dimensional form $z_0^{(410)} = 0.38$, $z_0^{(660)} = 0$, $w^{(l)} = 0.05$, $\gamma^{(410)} = 2.55 \times 10^9$, $\gamma^{(660)} = -2.55 \times 10^9$, $T_0^{(410)} = 0.92$, $T_0^{(660)} = 0.99$, and in (1)

$$\Gamma_x^{(l)} = -(\delta\rho^{(l)} \times \gamma^{(l)} / 2 \times \rho \times Ra^{(l)} \times w^{(l)}) \times T_x \times ch^{-2} \{[z - z_o^{(l)} + \gamma^{(l)} \times (\delta\rho^{(l)} / \rho \times Ra^{(l)}) \times (T - T_o^{(l)})] / w^{(l)}\} \quad (12)$$

Equations (1)–(2) are solved for the isothermal horizontal and vertical boundaries regarded no-slip impenetrable ones except for the "windows" for in-

and outgoing subducting plate, where the plate velocity is specified. Vertical boundary distant from subduction zone is assumed penetrable at right angle, the latter boundary condition appears not too imposing in the case of rather flat subduction of Amur Lithospheric Plate. Q in (2) is non-zero in the continental and oceanic crust 40 and 7 km thick. Initial vertical boundaries temperature is calculated for the half-space cooling model for 10^9 yr and 10^8 yr for Okhotsk (continental) and Amur Lithospheric Plates respectively. Additional alternative computation was performed for the Okhotsk Lithospheric Plate age of 10^8 yr.

Results and Discussion

Assuming the heat flux q maximum in [19] to be localized above the convective flow ascending from the mantle wedge to the Earth's surface at the Okhotsk seafloor and the convective 2D cell size is equal to the characteristic transversal size of the zone of anomalous heat flux, the convection cell dimension can be estimated as ~ 300 km.

To compute an accurate consistent model of small-scale convection in the mantle wedge between the overriding Okhotsk Lithospheric Plate and subducting Amur Lithospheric Plate it is necessary from the computational point of view first to specify in (1)–(2) vanishing non-dimensional numbers $Ra \to 0$, $Di=0$, i.e. to ignore convection and viscous dissipation. This approach is applied as convection with Ra and Di (4) passes through very vigorous stages, and the time steps in integrating (1)–(2) become too small thus making it difficult to model the thermal structure of micro plates. Solving (1)–(2) by the finite element method in space on the grid 104×104 and the 3-rd order Runge-Kutta method in time one obtains for $Ra \to 0$, $Di=0$ and $V=10$ mm per year non-dimensional quasi steady-state ψ and $T = T_R$ shown in Figs. 2, 3, where the streamlines are depicted in Fig. 2 with the step 5 and the isotherms in Fig. 3 with an interval 0.05.

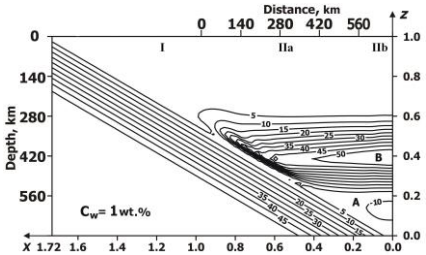

Fig. 2. Quasi steady-state non-dimensional stream-function distribution in the zone of subduction of the Amur Lithospheric Plate (I) under the Okhotsk one (IIa and IIb) for non-Newtonian rheology without effects of dissipative heating and convection not taken into account along the Harbin-Okha profile. The streamlines are depicted with a step 5. The distance along the upper boundary counts from the mantle "edge" of mantle wedge confined within the angle of 30º. Parallel equidistant streamlines represent the rigid subducting Amur Lithospheric Plate, the streamlines above correspond to the mantle wedge flows: primary one "A" and secondary "B" induced by subduction (flow "A") and by the flow "A". Induced flow "B" moves oppositely to subducting Amur Lithospheric Plate.

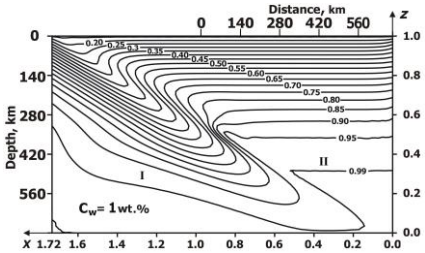

Fig. 3. Quasi steady-state non-dimensional temperature distribution in the zone of subduction of the Amur Lithospheric Plate (I) under the Okhotsk one (II) without effects of dissipative heating and convection taken into account for non-Newtonian rheology along the Harbin-Okha profile. The isotherms are depicted with a step 0.05. The distance along the upper boundary counts from the mantle "edge" of mantle wedge confined within the angle of 30º.

Subducting plate was considered rigid, while the viscosity at the zone of plate friction (at temperatures below 1200º*K*) was reduced by 2 orders of magnitude as compared to (5). The latter viscosity reduction at the plates contact zone accounts for lubrication effected by deposits partially entrained by the subducting plate. Such a lubrication prevents the overriding Okhotsk Lithospheric Plate from gluing to the subducting Amur one [5]. It is worth noting the isotherm $T = 0.15$ in Fig. 3 approximately corresponding to the Earth's surface is depressed at subduction zone by ~ 7 km which is of the order of a typical trench depth. Figures 2 and 3 show the results of computation for formulae (7) – (9) for the non-Newtonian rheology case (for the water content C_w increased from $C_w = 10^{-3}$ wt. % to $C_w = 1$ wt. %) since in the case of Newtonian rheology the convection in the mantle wedge is not aroused. The distance along the upper horizontal axis in Figs. 2 and 3 counts from the "edge" of mantle wedge. Figure 2 shows the return flow in the mantle wedge to be induced in the form of two vortices "A" and "B" located one above another, of which the upper one "B" (with $\psi > 0$) rotates clockwise and the lower one "A" (with $\psi < 0$) counter clockwise. The zone of friction of the induced flow "B" with the subducting Amur Lithospheric Plate is characterized by the great strain rate, thus the viscosity (7) drops there by several orders of magnitude and the initiation of an ascending flow of the Karig vortex becomes possible. The opposite flow "B" in Fig. 2 is obviously aroused by the flow "A" induced by subducting Amur Lithospheric Plate.

Assuming $Ra = 6.62 \times 10^8$ and $Di = 0.175$ according to (4), i.e. switching on dissipation and convection, and taking into account the effects of phase transitions, from (1)–(2) the convection is found to be aroused in the non-Newtonian rheology case at $C_w = 1$ wt. % in the form of 2 vortices (a single convective cell, shown in (Fig. 4) and initial flows in Fig. 2 to be destroyed during the non-dimensional time of 0.15×10^{-7} (in dimensional form 10^4 yr).

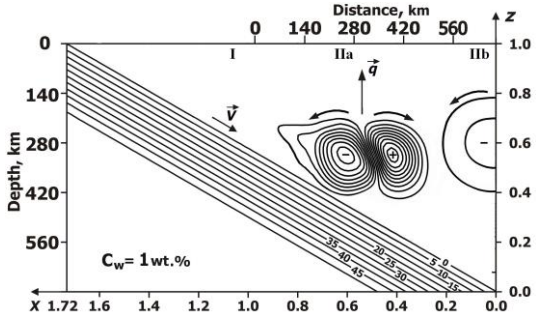

Fig. 4. Non-dimensional perturbed stream-function distribution in the zone of subduction of the Amur Lithospheric Plate (I) under the Okhotsk one (IIa and IIb) with the effects of dissipative heating and convection taken into account for non-Newtonian rheology and the water content C_w = 1 wt.% in the mantle wedge along the Harbin-Okha profile. The streamlines in convective vortices are depicted with a step of 2×10^6. Parallel equidistant streamlines represent the rigid subducting Amur Lithospheric Plate. Vector $\vec{q}$ indicates the direction of possible heat and calcareous-alkaline magmas transport from the mantle wedge to the Okhotsk seafloor. The signs "+" and "–" denote positive and negative stream function.

Whirl streamlines depicted with an interval of 2×10^6, actually correspond to convective cell dimension of ~ 300 km, while the streamlines density corresponds to convection velocity over ~10 m×yr^{-1}. Convection cell dimension of ~ 300 km is close to the spatial horizontal scale of heat flux anomaly observed in the Okhotsk Sea eastward of Sakhalin [19]. Fig. 5 shows an initial stage of formation of thermal diapir *D* ascending to the Earth's surface.

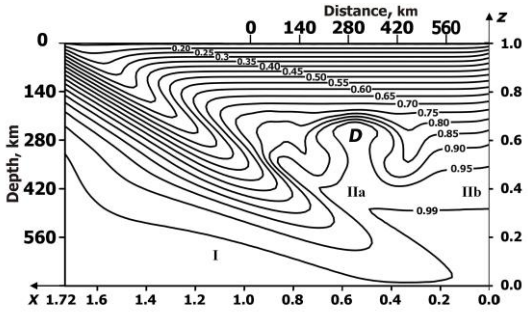

Fig. 5. Non-dimensional temperature at the initial stage of formation of a thermal diapir *D*, assuming the characteristic shape of a "mushroom" above the surface of subducting Amur Lithospheric Plate (I) and ascending to the base of overlying Okhotsk Lithospheric Plate (IIa and IIb) due to effects of viscous dissipation and convection along the Harbin-Okha profile.

The final stage of ascending micro whirls and corresponding isotherms are shown in Fig. 6, in which practically isothermal convective micro whirls at a temperature T_c = 0.525 (or. in a dimensional form, T_c ~10^3 *K*) are depicted with the interval 4, corresponding to the velocity V_c of the order of several tens of mm per year.

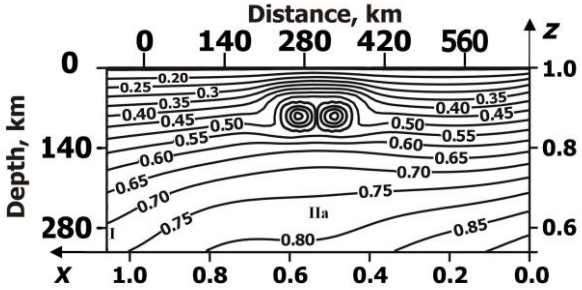

Fig. 6. The distributions of non-dimensional temperature (isotherms depicted with an interval 0.05) and stream-function (vortices with an interval 4) at the stage of maximum invasion of the thermal diapir into the Okhotsk Lithospheric Plate (IIa) along the Harbin-Okha profile. The diapir is nearly isothermal (with the temperature of ~10^3 *K*). Maximum convective heat flux of ~10^3 mW×m^{-2} over the convection cell centre is redistributed across the convection cell breadth and provides the surface heat flux of ~ 130 mW×m^{-2} from the Okhotsk seafloor in a distance of ~ 280 km eastward of the Sakhalin Island.

Thus the maximum convective heat flux is $q_c \sim \rho_m c_p T_c V_c \sim 10^3$ mW×m^{-2}, which is redistributed across the convective cell breadth forming the increase in the isotherms density, corresponding to the surface heat flux anomaly of ~ 130 mW×m^{-2}. This heat flux fits well to the value observed in the quasi 2D zone of heat flux anomaly eastward of Sakhalin [19]. It should be underlined that convective micro vortices, ascending to the base of the Okhotsk Lithospheric Plate (II) and penetrating into it, shown in Fig. 6, correspond to a non-steady state stage of convective instability, since thermal diapirs are forming at the upper surface of subducting Amur Lithospheric Plate (I) (see Fig. 5) and ascending to the Earth's surface during ~ 10^6 yr. Further on the process of formation and ascent of thermal diapirs is repeated quasi periodically. Rather fast an ascent of a thermal diapir in the non-Newtonian upper mantle at the ascent velocity of ~1 m×yr^{-1} is due to the local decrease in viscosity around the micro vortices because of the local viscous stress concentration.

It is worth noting that in the case of Newtonian rheology the mantle wedge dissipation-driven convection in the form of transversal rolls as in Fig. 4 is characteristic of very small subduction angles the convection of this type being absent already at subduction angle β = 30° at *V*=100 mm×yr^{-1} [3]. At the subduction angle under consideration here, β = 30°, the convective transversal rolls appear at $V > 200$ mm×yr^{-1}in the case of Newtonian rheology. In the case of non-Newtonian rheology the dissipation-driven convective transversal Karig's vortices can be aroused at sufficiently low subduction velocity and rather steep subduction. Arrow $\vec{q}$ above the boundaries of the oppositely revolving convective vortices shown in Fig. 4 for the non-Newtonian rheology case indicate possible direction of transport of non-organic mantle hydrocarbons to the Earth's surface. Thus the model constructed here favors the non-Newtonian mantle wedge rheology as better fitting to the observed heat flux anomaly localization, horizontal size and heat flux absolute value It should be noted that numerous thermo-mechanical mantle models

in the zones of subduction (see, e.g. [4; 5] and the vast number of references there) showed convection in the form of transversal rolls never to occurre as the models with extremely small subduction angle and sufficiently great subduction velocity were not investigated. For the non-Newtonian rheology case the 2D dissipation driven convection is aroused at V =10 mm×yr^{-1} and mean water content of $C_w \sim 1$ wt. % is owing to the 2 unperturbed induced flows ("A" and "B" in Fig. 2) one over another as well as to considerable viscous dissipation in the zone of friction of the upper flow "B" with the oppositely moving subducting Amur Lithospheric Plate (I). It should be underlined that the 2-layered structure of the flow induced in the mantle wedge by subducting Amur Lithospheric Plate appears in the non-Newtonian mantle rheology case only, and it is in this case that the localized zone of friction is formed where the subducting Amur Lithospheric Plate contacts the oppositely moving flow "B". Here the dissipative heat release becomes sufficient to originate an ascending convective flow shown by the vector q in Fig. 4. The non-Newtonian rheology predominates in the mantle wedge probably because of the great water content, supplied to there from subducting slab. The mantle effective viscosity drops with water content exclusively in the non-Newtonian mantle rheology case.

Additionally a computation was performed for the case of oceanic type of the Okhotsk Lithospheric Plate (IIa and IIb) of the age of 10^8 yr, in which case the 2D convection in the mantle wedge assumes the form shown in Fig. 7 with much broader horizontal convection cell dimension as compared to that shown in Fig. 4 for the continental type of the Okhotsk Lithospheric Plate.

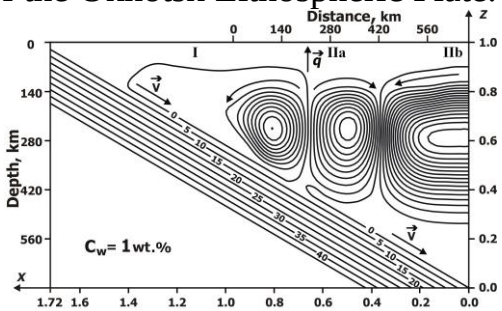

Fig. 7. Non-dimensional perturbed stream-function distribution in the zone of subduction of the Amur Lithospheric Plate (I) under the Okhotsk one (IIa and IIb) with the effects of dissipative heating and convection taken into account for non-Newtonian rheology, water content C_w = 1 wt.% in the mantle wedge as in Fig. 4 for Okhotsk Lithospheric Plate along the Harbin-Okha profile. Greater than in Fig.4 convection cell dimension far exceeds the horizontal scale of the observed heat flux anomaly zone to the east of Sakhalin.

The zone of anomalous heat flux becomes also much broader than it is observed actually according to [19]. Thus this extra computation favors the concept of continental type of the Okhotsk Lithospheric Plate in accordance with [13], where the deep seismic sounding profiles made with a very detailed system of observation are shown to ultimately decide the problem of the Okhotsk Sea crustal type as that of a typical continental crust one with a thick granite-gneiss layer, and the upper mantle velocity models along with the deep seismic sounding profiles are

as well shown to be similar to continental ones. In [op. cit.] the Okhotsk Sea Basin is as well indicated to be the most prospective gold-bearing regions of the world.

Figs. 4 and 5 show the temperature profiles as a function of depth, which profiles along with the data on the mantle pressure distribution beneath the Okhotsk Lithospheric Plate in [25] support the idea that under the condition of mantle serpentization plastic serpentinized rocks at depths of 40 km (at $T > 700^oK$ – 900^oK and $P > 13 – 15$ kbar) form thermal diapirs, which result from adiabatic upwelling to the surface crust layers and consequent decompression of heated deep material, and it is with these diapirs that the calcareous-alkaline magmas supply is associated [17]. In other words, the layers of serpentinized rocks may be considered to accumulate calcareous-alkaline magmas ascending from mantle, thus creating natural traps for alkali metals and gold. A large number of the earthquake foci in the fore-arc zones results in a destruction of the integrity of the serpentinite rock layers, where significant deposits of alkali metals and gold are accumulated. This forces calcareous-alkaline magmas to intrude into the subsurface sedimentary rock layers along the tectonic faults located in the zones of subduction rise above the zones of thermal diapirs. Such a prospective area for the search for gold ore deposits is located in Amur region and the Okhotsk Sea by the northeastern end of the Sakhalin Island (Fig. 8).

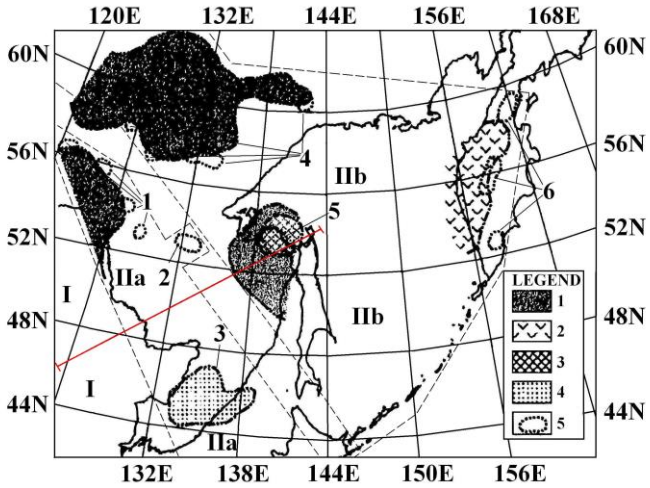

Fig. 8. A map of quasi-linear projection zones on the Earth's surface of the locations of deep-lying plumes (mantle diapirs) and associated gold ore deposits (1-6) in the Okhotsk Lithospheric Plate (IIa and IIb) [9]. I - Amur Lithospheric Plate; II - Okhotsk Lithospheric Plate; two quasi-linear zones (IIa and IIb) of two chains of mantle plumes (thermal diapirs) on the territory of the Okhotsk Lithospheric Plate are highlighted with dashed lines; Gold ore deposits: 1 – Pokrovsko-Berezitovy; 2 – Bam; 3 – Ussuri; 4 – Central Aldan; 5 – Ket-Cape; 6 – Kamchatka; Legend: projections of zones of mantle diapirs with ascending and descending hydrothermal flows of calcareous-alkaline composition on the Earth's surface: 1 – descending flows; 2 – ascending flows; 3 – mixed, mainly descending flows; 4 – mixed, mainly ascending flows; 5 – contours of already exploited gold ore deposits in the Okhotsk Lithospheric Plate (near Sakhalin Island); red line is the location of the Harbin-Okha profile.

The rectangle on the map in Fig. 8 encompasses the Okhotsk Lithospheric Plate where several gold ore deposits (1 - 6) are revealed at the site of rise of the mantle diapirs confirms that the search for gold deposits at the areas of ascent of mantle diapirs in subduction zones is of a reasonable prospect, as is illustrated here. In the Amur-Okhotsk region (Fig. 8), two linear zones (IIa and IIb) are visible, almost parallel to each other, within which there are deposits of alkali metals and gold (1-3 and 4-6) located at a distance of about 400-500 km, which corresponds to the calculations carried out in the article. The formation of a chain of ore mineral deposits (in particular, deposits of alkali metals and gold) on the territory of the Amur-Okhotsk region was facilitated by multiphase magmatic activity, volcanism and the rise of calcareous-alkaline magmas with various metals dissolved in them, which arose above the Karig mantle convective vortices in the Amur-Okhotsk subduction zone. Under the action of convective vortices, molten magma rose through numerous cracks and faults in the crust of the Amur-Okhotsk region. The sublatitudinal distribution of various deposits of metal ores parallel to each other on the territory of the Amur-Okhotsk region with a distance of about 400-500 km between them confirms the results of studies related to the sublatitudinal arrangement of the Karig roller (quasi-cylindrical) convective vortices that arose during geological evolution in the subduction zone of the Amur Lithospheric Plate.

Conclisions

In the non-Newtonian mantle rheology case the convection cell dimension in the mantle wedge formed as the result of subduction of Amur Lithospheric Plate under the Okhotsk one amounts to ~ 300 km for the velocity of subduction of 10 mm per year. This convection cell size roughly coincides with the characteristic size of the 2D zone of anomalous heat flux observed at the Okhotsk seafloor eastward of the Sakhalin Island. Thermal diapir ascending from the surface of subducting Amur Lithospheric Plate contains convective micro whirls, reaches the depth of ~ 40-90 km and can provide the anomalous heat flux of ~ 130 $mW \times m^{-2}$ actually observed to the east of Sakhalin. Thermo-tectonic model of mantle wedge presented here for the angle and velocity of subduction of 36º и 10 mm per year respectively fits well to the results of the most recent GPS observations as well as to the observed anomalous heat flux and location and horizontal extent of the zone of heat flux anomaly eastward of Sakhalin thus being a convictive argument in favor of the eastward Amur Lithospheric Plate subduction and the continental type of the Okhotsk Lithospheric Plate. The model predicts the calcareous-alkaline magmas zone to be localized Amur region and eastward of Sakhalin at the anomalous heat flux zone.

References

1. Billen M., Hirth G. Newtonian versus non-Newtonian Upper Mantle Viscosity: Implications for Subduction Initiation. Geophys. Res. Lett. 2005. V.32. (L19304). doi: 10.1029/2005GL023458.

2. Gavrilov S.V. Investigation of the island arc formation mechanism and the back-arc lithosphere spreading. Geophysical Researches. 2014. V. 15. No. 4. pp. 35–43.

3. Gavrilov S.V., Abbott D.H. Thermo-mechanical model of heat- and mass-transfer in the vicinity of subduction zone. Physics of the Earth. 1999. V.35. No.: 12. pp. 967–976.

4. Gerya T.V. Future directions in subduction modeling. J. of Geodynamics. 2011. V.52. pp. 344-378. doi:10.1016/j.jog.2011.06.005

5. Gerya T.V., Connolly J.A.D., Yuen D.A., Gorczyk W., Capel A.M. Seismic implications of mantle wedge plumes. Phys. Earth Planet. Inter. 2006. V.156. pp. 59-74. doi: 10.1016/j.pepi.2006.02.005

6. Ismail-Zadeh A., Honda S., Tsepelev I. Linking mantle upwelling with the lithosphere decent in the Japan Sea evolution: a hypothesis. Scientific Reports. No. 3. pp. 1137. http://dx.doi.org/101038/srep01137.

7. Karig D.E. Origin and development of marginal basins in the Western Pacific. Journal Geophysical Researches. 1971. V.76. No. 11. pp. 2542-2561. doi: 10.1029/JB076i011p02542

8. Katsumata K., Kasahara M., Ichivanagi M., Kikuchi M., Sen R.-S., Kim Ch.-U., Ivaschenko A., Tatevossian R. The 27 May 1995 Ms 7.6 Northern Sakhalin Earthquake: An Earthquake on an Uncertain Plate Boundary. Bulletin of the Seismological Society of America. 2004. V.94. No. 1. pp. 117 – 130.

9. Khanchuk A.I., Ivanov V.V. Meso-Cenozoic geodynamic conditions and gold mineralization of the Russian Far East. Geology and geophysics. 1999. Vol. 40. No. 11. pp. 1635-1645.

10. Kogan M.G., Burgmann R., Vasilenko N.F., Scholtz C.H., King R.W., Ivashchenko A.I., Frolov D.I., Steblov G.M., Kim Ch.U., Egorov S.G. The 2000 Mw 6.8 Uglegorsk earthquake and regional plate boundary deformation of Sakhalin from geodetic data. Geophys. Res. Lett. 2003. V.30. No.3. pp. 1102 - 1106. doi: 10.1029/2002GL016399.

11. Kogan M.G., Steblov G.M. Current global plate kinematics from GPS (1995 – 2007) with the plate-consistent reference frame. J. Geophys. Res. 2008. V.113. pp. 1 – 17. B04416. doi:10.1029/2007JP.O05353.

12. Noble J. A. Metal provinces and metal finding in the western United States. Bull. Geol. Soc. Am. 1970. V. 81. pp. 1607-1624.

13. Pavlenkova N.I., Kashubin S.N., Gontovaya L.I., Pavlenkova G.A. Deep structure and geodynamics of the Sea of Okhotsk region. Regional geology and metallogeny. 2018. No.76. pp. 70 – 82.

14. Sawkins F.J. Sulfide ore deposits in relation to plate tectonics // Journ. Geol. 1972. V. 80. No. 4. pp. 377-397.

15. Schubert G., Turcotte D.L., Olson P. Mantle Convection in the Earth and Planets. New York: Cambridge University Press, 2001. 940 p.

16. Seno T., Sakurai T., Stein S. Can the Okhotsk plate be discriminated From the North American plate? J. Geophys. Res. V. 101. pp. 11,305–11,315.

17. Sillitoe R.H. Relation of metal provinces in Western America to subduction of oceanic lithosphere. Bull. Geol. Soc. Am. 1972. V. 83. pp. 813-818.

18. Sim L.A., Bogomolov L.M., Bryantseva G.V., Savvishev P.A. Neotectonics and tectonic stresses of the Sakhalin Island. Geodynamics & Tectonophysics. 2017. V.8. No.1. pp.181–202. DOI:105800/GT-2017-8-1-0237.

19. Smirnov Ya.B. (ed.) The Map of the Heat Flux at the Territory of the USSR and Adjacent Regions. Moscow: GUGK. 1980.

20. Sunuwar L, Cuadra C, Karkee M. B. Strong ground motion attenuation in the Sea of Japan (Okhotsk-Amur plates boundary) region. 13-th World Conference on Earthquake Engineering. Vancouver, B.C., Canada. August 1-6, 2004. Paper No. 197.

21. Taira, A. Tectonic evolutions of the Japanese island arc system. Ann. Rev. Earth Planet. Sci. 2001. V. 29. pp. 109-134.

22. Trubitsyn V.P., Trubitsyn A.P. Numerical model of formation of the set of lithospheric plates and their penetration through the 660 km boundary. Physics of the Earth. 2014. No. 6. pp. 138- 147.

23. Zharkov V.N. Physics of the Earth's Interiors. Duesseldorf: Lambert Academic Publishing. 2019. 438 p.

24. Zonenshain L.P., Savostin L.A. Geodynamics of the Baikal rift zone and plate tectonics of Asia. Tectonophysics. 1981. V. 76. pp. 1 – 45.

25. Yurkova R.M., Voronin B.I. Ascent and transformation of mantle hydrocarbon fluids in connection with a formation of ophiolite diapers. In: "The genesis of hydrocarbon fluids and deposits". Geos. 2006. pp. 56-67.